

# Detection of explosives on human nail using confocal Raman microscopy

Esam M. A. Ali, Howell G. M. Edwards,\* Michael D. Hargreaves and Ian J. Scowen

Trace amounts of explosives were detected on human nail using confocal Raman microscopy. Contamination of the nail can result from the manual handling, packaging or transportation of explosive substances. Raman spectra were obtained from pentaerythritol tetranitrate (PETN), trinitrotoluene (TNT), ammonium nitrate and hexamethylenetetramine (HMTA) particles on the surface of the nail with dimensions in the range 5–10  $\mu\text{m}$ . An added difficulty in an analytical procedure is the presence of a nail varnish coating that has been applied, which traps the particulate matter between the coating and nail. Using confocal Raman microscopy, interference-free spectra could be acquired from particles of explosives visually masked by the nail varnish. Spectra of the explosives could be readily obtained *in situ* within 90 s without alteration of the evidential material. Acquisition of a Raman point map of a PETN particle under the nail varnish coating is also reported. Copyright © 2008 John Wiley & Sons, Ltd.

**Keywords:** explosives; explosive precursors; human nail; Raman spectroscopy; forensic

## Introduction

The analysis of keratinized matrices, such as hair and nails, for drugs of abuse is now recognized as an important tool for forensic toxicologists. Advances in modern analytical instrumentation have enabled the analysis of drugs in these unconventional biological matrices to be accomplished.<sup>[1–5]</sup> Several studies in the literature have demonstrated that nail clippings can provide a readily accessible matrix for the postmortem detection of drugs of abuse; opiates, methamphetamine, cocaine and cannabis have been successfully detected in the nail clippings of drug abusers.<sup>[6–12]</sup> Furthermore, DNA extracted from debris of fingernails of victims of violent or aggressive acts has been used in the identification of the assailants.<sup>[13–15]</sup>

Several sophisticated analytical methods have been established for the identification of explosives under various conditions, including gas chromatography,<sup>[16]</sup> X-ray powder diffraction,<sup>[17]</sup> thermal neutron analysis,<sup>[18]</sup> ion mobility spectrometry,<sup>[19]</sup> and ionization desorption mass spectrometric methods.<sup>[20–22]</sup> However, many of these techniques involve the complete or partial destruction of the samples, often after sample preparation.

Modern technological advancements for the detection of Raman scattering have established the application of the technique in the field of forensic science.<sup>[23–25]</sup> Raman spectroscopy produces molecule-specific spectra and, in most cases, sample preparation is not necessary, allowing the nondestructive analysis of tablets, powders and liquids *in situ*. This is particularly important with regard to the speed of analysis, prevention of sample contamination and preservation of evidential material.<sup>[26]</sup> The international literature contains several publications addressing the application of Raman spectroscopy for the detection and identification of explosives. For example, Fourier transform (FT) Raman spectroscopy was successfully applied for the detection of explosive components in unknown Semtex samples.<sup>[27]</sup> *In situ* detection and identification of plastic explosives contained in fingerprint samples using Raman microscopy has been reported.<sup>[28]</sup> Also, a fiber optic probe for the

detection and identification of explosive materials has been developed, which has allowed Raman spectra to be acquired remotely from a spectrometer.<sup>[29,30]</sup>

With the use of excitation sources in the near-infrared (NIR), Raman spectroscopy could be applied for the characterization of the molecular structure of sensitive biomaterials such as skin, callus, hair and nail.<sup>[31]</sup> A comparative study of the FT-Raman spectra of mammalian and avian keratotic biopolymers (stratum corneum, human nail, feather and bull's horn) was carried out by Akhtar and Edwards.<sup>[32]</sup> Raman spectroscopy and multivariate classification techniques have been applied for the differentiation of finger nails and toe nails.<sup>[33]</sup> Recently, a novel method for human gender classification using Raman spectroscopy of finger nail clippings has been reported.<sup>[34]</sup>

The ability to identify visually obscured particles of forensic relevance affords significant advantages to the investigator. In earlier work in our laboratory, confocal Raman microscopy was applied for the detection of drugs of abuse in cyanoacrylate-fumed fingerprints,<sup>[35]</sup> and the technique could be successfully applied for detection and identification of drugs of abuse on the surface of human nail and under a coating of nail varnish.<sup>[36]</sup> Manual handling, packaging or transportation of explosive substances may result in contamination of the nail by these substances. Detection of residues of explosives on nail can be used as evidence to establish a link between these hazardous materials and the individuals involved in terrorist activities. In this present study, we extended the application of this approach to the detection of explosives and their precursors on the surface of human nail. An added

\* Correspondence to: Howell G. M. Edwards, Raman Spectroscopy Group, University Analytical Centre, Division of Chemical and Forensic Sciences, University of Bradford, Bradford BD7 1DP, UK. E-mail: H.G.M.Edwards@bradford.ac.uk

Raman Spectroscopy Group, University Analytical Centre, Division of Chemical and Forensic Sciences, University of Bradford, Bradford BD7 1DP, UK

difficulty in an analytical procedure is the presence of a nail varnish coating that has been applied, which traps the particulate matter between the coating and the nail; here we shall demonstrate the discrimination power of confocal Raman microscopy for the detection of explosives and explosive precursor substances on uncoated nail and also under a coating of nail varnish. Exploiting the high axial resolution of the confocal arrangement, interference-free spectra of explosives could be acquired from particles visually masked by the nail varnish. Furthermore, the application of Raman mapping techniques allows visualization of particle morphology in obscured settings and obtaining the spatial distribution of a given compound within a heterogeneous specimen. This investigation establishes the utility of these Raman spectroscopic techniques in this context and establishes the technique of *in situ* Raman mapping as a useful tool for the forensic analysis of hazardous materials.

## Experimental

### Samples

Pentaerythritol tetranitrate (PETN), trinitrotoluene (TNT) and ammonium nitrate samples were supplied by the Home Office Scientific Development Branch. Hexamethylenetetramine (HMTA), a chemical precursor used in the manufacture of high explosives such as cyclotrimethylenetrinitramine (RDX), used in this study was supplied by Sigma–Aldrich Company Ltd., United Kingdom.<sup>[37]</sup>

Finger nail clipping samples were donated from the authors. A red nail varnish (GC, Procter & Gamble, “Nail Slicks Well Red 141, Rouge Expert”) was purchased from a local store. The nail clippings were doped with few crystals of the explosive substances. Raman spectra were collected from individual crystals of dimensions in the range of 5–10  $\mu\text{m}$  on the surface of the nail. A single layer of the nail varnish was then applied to the doped nails and spectra of the crystals of the explosives under the nail varnish coating were collected. A Raman point map was also acquired from a PETN crystal under the nail varnish coating.

### Raman spectroscopy

Reference Raman spectra of samples of explosives, nail and nail varnish were obtained to be used as reference spectra for comparison with the spectra of the particles of explosives on the surface of the nail and under the nail varnish. Raman spectra were collected using a Renishaw InVia Reflex dispersive Raman microscope (Wotton-under-Edge, UK). The Raman spectra were excited with a 785-nm NIR diode laser [Renishaw HPNIR laser (Renishaw, Wotton-under-Edge, UK)] and a 50 $\times$  objective lens, giving a laser spot diameter of 2  $\mu\text{m}$ . Spectra were obtained at 2  $\text{cm}^{-1}$  resolution for a 10 s exposure of the charge-coupled device (CCD) detector in the wavenumber region 100–1800  $\text{cm}^{-1}$  using the extended scanning mode of the instrument. With 90.8 mW laser power at the sample, only one accumulation was necessary for the explosive samples and five accumulations for both the nail and nail varnish. The total acquisition time of the spectra of the explosives was 90 s. Spectral acquisition, presentation and analysis were performed with the Renishaw WIRE (service pack 9) and GRAMS AI version 8 (Thermo Electron Corp., Waltham, MA, USA) software.

A depth profile was obtained from a PETN particle coated with the nail varnish. Spectra were collected from the nail varnish coating ( $Z = 0 \mu\text{m}$ ) and by incrementally moving the laser focus

in 20  $\mu\text{m}$  intervals through the PETN particle to the nail substrate using the graduated fine-focus adjustment of the microscope. Also, a Raman point map ( $\sim 30 \times 30 \mu\text{m}$  map area) was acquired for a PETN crystal under the nail varnish. Using a 50 $\times$  objective, a Raman map was obtained by collecting spectra with 10 s exposure time and subsequently moving the sample in a raster pattern with a step size of 2  $\mu\text{m}$ . Data acquisition covered the spectral range 100–1800  $\text{cm}^{-1}$  with a spectral resolution of 2  $\text{cm}^{-1}$  with each exposure of the CCD detector. The laser intensity at the sample was reduced to 10.8 mW to avoid burning of the sample. The total acquisition time for the Raman map experiment was approximately 10 h.

## Results and Discussion

It was observed that the spectra obtained from the particles of explosives on the surface of the nail contained some bands arising from the nail substrate. In all case, the strongest bands arising from the nail substrate did not interfere with the identification of the explosives, as these bands did not overlap with the characteristic Raman bands of the explosives. Figure 1 shows the image of a PETN crystal of several micrometers in size on the surface of the nail, and Fig. 2(a) shows the Raman spectrum obtained from this crystal. Comparison of this spectrum with the reference spectrum showed that PETN could be easily identified by its Raman spectrum, which comprises strong, sharp features in the fingerprint region of the spectrum. The Raman spectrum of PETN has several characteristic features of nitrate ester explosives that can be used to identify it: the symmetric ( $\text{NO}_2$ ) stretching mode at 1290  $\text{cm}^{-1}$ , the (O–N) stretching mode at 871  $\text{cm}^{-1}$  and the (C–C–C) deformation mode at 622  $\text{cm}^{-1}$ .<sup>[38]</sup> PETN could be identified from these strong bands, and through careful confocal sampling; no significant peaks in the spectrum appear from the nail substrate. A confocal spectrum obtained from a TNT crystal on the surface of the nail [Fig. 3(a)] shows that the explosive could be readily identified. The Raman spectrum of TNT contains several diagnostic features such as the  $\nu_{\text{as}}(\text{NO}_2)$  at 1532  $\text{cm}^{-1}$ , the  $\nu_{\text{s}}(\text{NO}_2)$  at 1357  $\text{cm}^{-1}$  and the ( $\text{NO}_2$ ) scissoring mode at 822  $\text{cm}^{-1}$ .<sup>[39]</sup> Despite the fact that the TNT spectrum contains two very weak bands arising from the nail, the amide I (C=O) mode at 1650  $\text{cm}^{-1}$  and the  $\delta(\text{CH}_2)$



**Figure 1.** PETN crystal on the surface of human nail. This figure is available in colour online at [www.interscience.wiley.com/journal/jrs](http://www.interscience.wiley.com/journal/jrs).

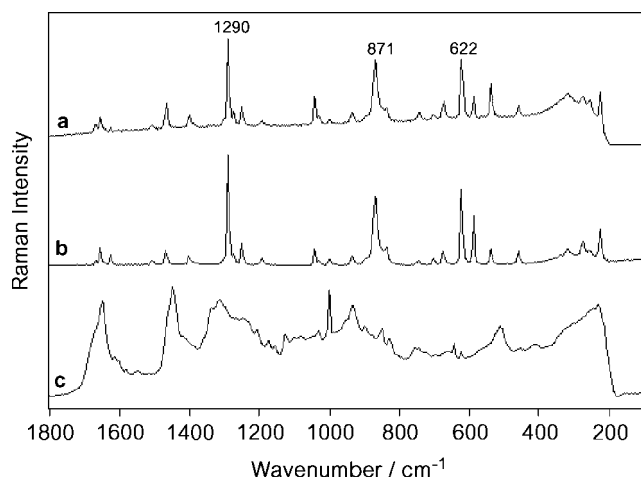


**Figure 2.** Raman spectra of (a) PETN on the surface of the nail (b) reference PETN (c) human nail. All spectra are of 785 nm excitation, 10 s exposure, one accumulation for (a) and (b) and five accumulations for (c).

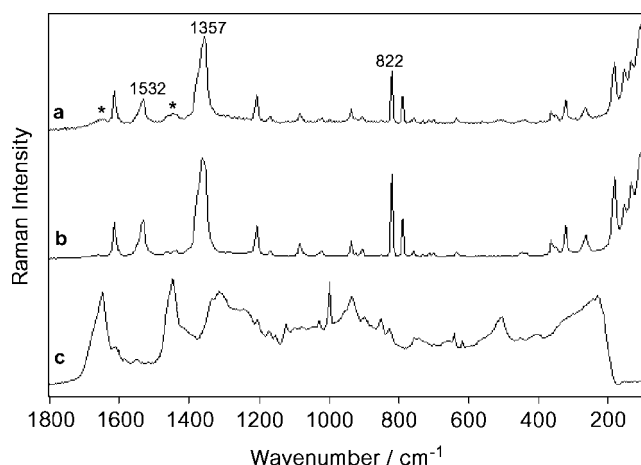


**Figure 3.** Raman spectra of (a) TNT on the surface of the nail (asterisks indicate nail bands) (b) reference TNT (c) human nail. All spectra are of 785 nm excitation, 10 s exposure, one accumulation for (a) and (b) and five accumulations for (c).

mode at  $1445\text{ cm}^{-1}$ ,<sup>[40]</sup> these nail bands do not overlap with the characteristic bands of the explosive. Also, a spectrum obtained from an ammonium nitrate crystal embedded on the surface of the nail (Fig. 4(a)) contains some bands arising from the nail: the amide I ( $\text{C}=\text{O}$ ) at  $1650\text{ cm}^{-1}$  and the  $\delta(\text{CH}_2)$  mode at  $1445\text{ cm}^{-1}$ . The presence of these nail bands did not prevent identification of ammonium nitrate, which could be done by its very strong  $(\text{NO}_3)^-$  stretching mode at  $1040\text{ cm}^{-1}$  and the  $(\text{NO}_3)^-$  bending mode at  $712\text{ cm}^{-1}$ .<sup>[41]</sup> Similarly, a Raman spectrum obtained from an HMTA crystal on the surface of the nail is shown in Fig. 5(a). It is observed that the amide I ( $\text{C}=\text{O}$ ) mode assigned to the nail substrate appears as a broad, weak band at  $1650\text{ cm}^{-1}$ . The presence of this band did not interfere with the identification of the explosive precursor HMTA, which could be easily identified by several characteristic signature bands such as the strong ( $\text{N}-\text{C}-\text{N}$ ) bending modes at  $1040$  and  $462\text{ cm}^{-1}$  and the very strong ( $\text{N}-\text{C}$ ) stretching mode at  $777\text{ cm}^{-1}$ .<sup>[42]</sup>

Raman spectra could be acquired from explosive particles on the surface of the nail with dimensions in the range  $5\text{--}10\text{ }\mu\text{m}$ . The

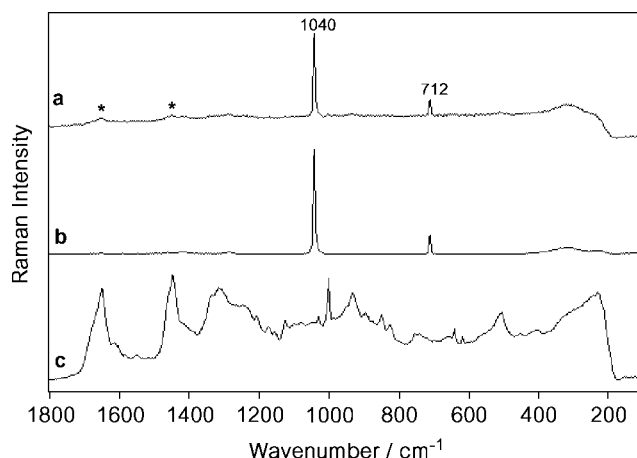


**Figure 4.** Raman spectra of (a) ammonium nitrate on the surface of the nail (asterisks indicate nail bands) (b) reference ammonium nitrate (c) human nail. All spectra are of 785 nm excitation, 10 s exposure, one accumulation for (a) and (b) and five accumulations for (c).

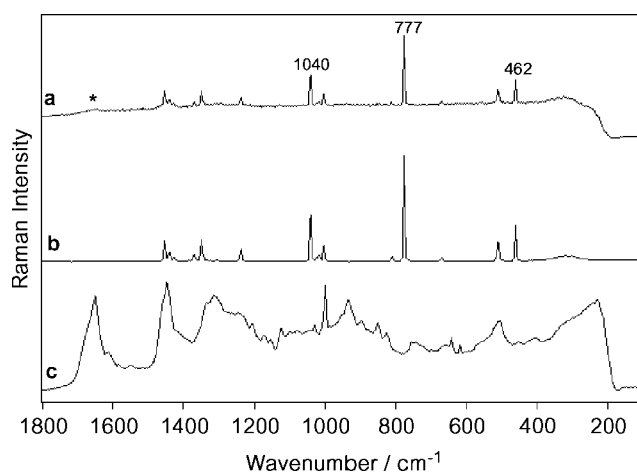


**Figure 5.** Raman spectra of (a) HMTA on the surface of the nail (asterisks indicate nail bands) (b) reference HMTA (c) human nail. All spectra are of 785 nm excitation, 10 s exposure, one accumulation for (a) and (b) and five accumulations for (c).

spectra are of high quality with a good signal/noise ( $S/N$ ) ratio, and there was no appreciable background due to fluorescence. Confocal Raman microscopy was applied to focus the laser beam and collect the Raman scattering from crystals of the explosives on the surface of the nail. Interference from the nail, including background fluorescence, was overcome by carefully focusing the confocal beam, and the resulting spectra allowed ready differentiation of interference from bands of the nail substrate. In addition, the NIR laser at 785 nm gave excellent spectra of the explosives and there was no detectable background fluorescence. This high discrimination power of the confocal microscope is attributed to the ability of such a system to isolate the light originating from a small region of the sample coincident with the focal point, which efficiently eliminates the contribution from out-of-focus zones, thereby making their Raman signals negligible.

Figure 6 shows an image of a PETN crystal obscured by nail varnish. The incident laser radiation was focused with the microscope objective onto this crystal, and the collected Raman spectrum is displayed in Fig. 7(b). Comparing the spectrum of PETN under the



**Figure 6.** PETN crystal under nail varnish. This figure is available in colour online at [www.interscience.wiley.com/journal/jrs](http://www.interscience.wiley.com/journal/jrs).

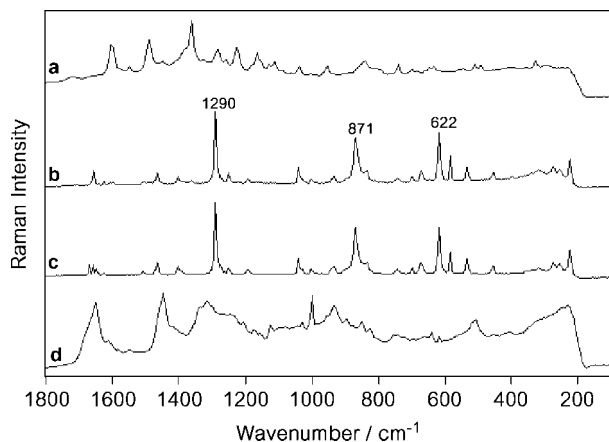


**Figure 7.** Raman spectra of (a) nail varnish (b) PETN under nail varnish (c) reference PETN (d) human nail. All spectra are of 785 nm excitation, 10 s exposure, five accumulations for (a) and (d) and one accumulation for (b) and (c).

nail varnish with the reference spectrum, it is clearly observed that PETN could be identified, and there are no significant peaks in the spectrum that are clearly attributable to either the nail or nail varnish. Although the crystal of the explosive is sandwiched between the highly fluorescent nail varnish and the nail substrate, the Raman spectrum could be obtained without interference from these highly fluorescent matrices. Further illustrations of the applicability of this approach were obtained from TNT, ammonium nitrate and HMTA particles covered by nail varnish (Fig. 8). These spectra are of high S/N ratio, with no detectable background fluorescence. The characteristic bands of the explosive substances could be clearly identified in these spectra, and no significant band could be assigned to either the nail varnish coating or the nail substrate. Coating of the explosive particles with the nail varnish presented no difficulty in determining the identity of the explosive substances, which could be attributed to the explosives having good Raman scattering cross-sections and the limited confocal scattering volume. This clearly demonstrates the major advantage of confocal Raman microscopy, namely, the ability to focus the incident laser radiation onto and collection of Raman scattering from a small point within the interior of a larger, highly fluorescent sample.

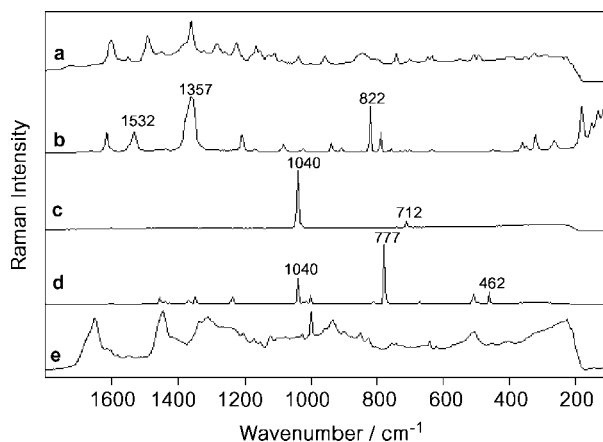


**Figure 8.** Raman spectra of (a) nail varnish (b) TNT under nail varnish (c) ammonium nitrate under nail varnish (d) HMTA under nail varnish (e) human nail. All spectra are of 785 nm excitation, 10 s exposure, five accumulations for (a) and (e) and one accumulation for (b), (c) and (d).

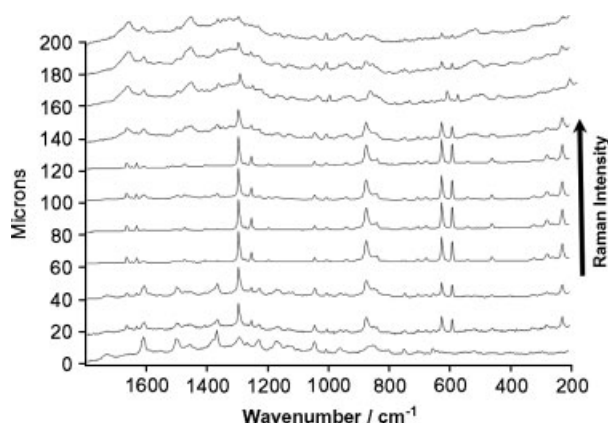


**Figure 9.** Confocal depth profile of a PETN particle coated with nail varnish. Spectra were collected from the nail varnish coating ( $Z = 0 \mu\text{m}$ ) and at  $20\text{-}\mu\text{m}$  intervals through the PETN particle down to the nail substrate.

Further illustrations of the depth discrimination capability of the confocal approach are demonstrated in Fig. 9, where a PETN particle under a nail varnish coating was depth-profiled. Spectra were collected from the nail varnish coating ( $Z = 0 \mu\text{m}$ ) and then at  $20\text{-}\mu\text{m}$  intervals through the PETN particle down to the nail substrate using the graduated fine-focus adjustment of the microscope. These spectra show that the three layers are clearly distinguishable and distinctive spectra could be obtained from the nail varnish coating, the explosive contaminant and nail substrate.

Raman mapping was carried out using the WIRE 2 software, allowing an area of the sample to be selectively investigated; a point map could be acquired from a PETN particle obscured by the nail varnish (Fig. 10(a)). Data were collected in an XY raster pattern and processed using band intensity, position, area, etc. In this case, a band from the analyte, the  $1290\text{ cm}^{-1}$  [symmetric ( $\text{NO}_2$ ) stretching], was chosen that was not affected by other species in the matrix. This band was curve-fitted using WIRE 2, and the mapping data was processed with this curve-fit to give a false color image of the PETN particle (Fig. 10(b)). The Raman point map shows that the PETN particle could be clearly located under the nail varnish. Though time consuming ( $\sim 10\text{ h}$ ), the technique

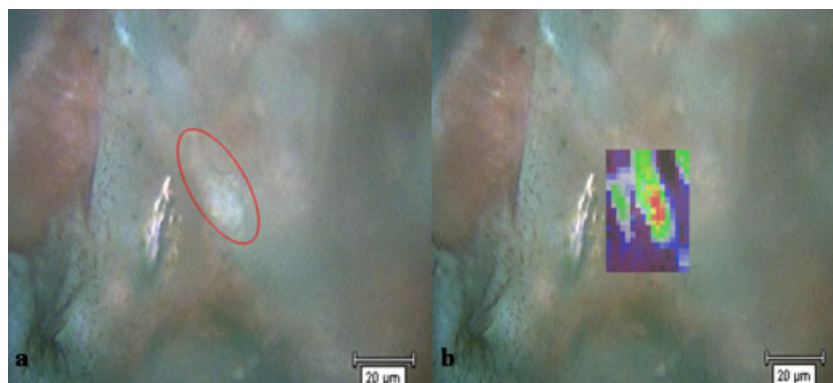


**Figure 10.** (a) Video image of a PETN crystal under nail varnish (b) Raman point map of PETN crystal under nail varnish (acquired using the  $1290\text{-cm}^{-1}$  peak area): low peak area in blue, high peak area in red. This figure is available in colour online at [www.interscience.wiley.com/journal/jrs](http://www.interscience.wiley.com/journal/jrs).

provides an overview of the spatial distribution of the particles of explosives under nail varnish.

These results demonstrate the discrimination power of confocal Raman microscopy in identifying explosives and explosive precursors on nails and under nail varnish. Raman spectra could be obtained from particles of explosives with dimensions in the range  $5\text{--}10\text{ }\mu\text{m}$ . The presence of a nail varnish coating on the particles presented no difficulty in determining the identity of the explosives substances. This ability for discrimination could be attributed to the ability of the confocal system to focus the incident laser radiation to obtain data nondestructively from particles under the coating. Consequently, the resulting Raman spectrum contains Raman signal almost exclusively from the focal point of the laser. Furthermore, the use of the NIR laser as an excitation source is an added advantage, as the generation of fluorescence is much reduced. These results confirm that the detection of explosives on nails can be used for security purposes or as a strong evidence to establish a link between these hazardous substances and individuals involved in possible terrorist activities.

## Conclusions

Confocal Raman microscopy can be an efficient technique for the detection and identification of residues of explosives in obscured situations. Interference-free Raman spectra as well as two-dimensional Raman map could be acquired from particles of explosives on the surface of the nail and under the coating of a nail varnish. The NIR laser gave excellent spectra of the explosives, and there was no appreciable fluorescence background. Selective Raman spectra of the explosives and their precursors were acquired *in situ* within 90 s with little or no sample preparation and without alteration or modification of the evidential material.

## Acknowledgements

The authors would like to thank the Egyptian Government for providing financial support to Esam M.A. Ali, Dennis Farwell for technical support and the Home Office Scientific Development Branch and the Forensic Science Service for providing the samples of explosives.

## References

- [1] R. C. Irving, S. J. Dickson, *Forensic Sci. Int.* **2007**, *166*, 58.

- [2] F. Musshoff, F. Driever, K. Lachenmeier, D. W. Lachenmeier, M. Banger, B. Madea, *Forensic Sci. Int.* **2006**, *156*, 118.  
[3] C. Gambelunghe, R. Rossi, C. Ferranti, R. Rossi, M. Bacci, *J. Appl. Toxicol.* **2005**, *25*, 205.  
[4] E. Cognard, S. Rudaz, S. Bouchonnet, C. Staub, *J. Chromatogr. B* **2005**, *826*, 17.  
[5] K. Lachenmeier, F. Musshoff, B. Madea, *Forensic Sci. Int.* **2006**, *159*, 189.  
[6] O. Suzuki, H. Hattori, M. Asano, *Forensic Sci. Int.* **1984**, *24*, 9.  
[7] N. P. Lemos, R. A. Anderson, J. R. Robertson, *J. Anal. Toxicol.* **1999**, *23*, 147.  
[8] D. A. Engelhart, A. J. Jenkins, *J. Anal. Toxicol.* **2002**, *26*, 489.  
[9] D. Garside, J. D. Roper-Miller, B. A. Goldberger, W. F. Hamilton, W. R. Maples, *J. Forensic Sci.* **1998**, *43*, 974.  
[10] N. P. Lemos, R. A. Anderson, R. Valentini, F. Tagliaro, R. T. Scott, *J. Forensic Sci.* **2000**, *45*, 407.  
[11] D. A. Engelhart, E. S. Lavins, C. A. Sutheimer, *J. Anal. Toxicol.* **1998**, *22*, 314.  
[12] S. Valente-Campos, M. Yonamine, R. L. de Moraes Moreau, O. A. Silva, *Forensic Sci. Int.* **2006**, *159*, 218.  
[13] D. A. Gangitano, M. G. Garofalo, G. J. Juvenal, B. Budowle, R. A. Padula, *J. Forensic Sci.* **2005**, *47*, 175.  
[14] T. D. Anderson, J. P. Ross, R. K. Roby, D. A. Lee, M. M. Holland, *J. Forensic Sci.* **1999**, *44*, 1053.  
[15] P. Wiegand, T. Bajanowski, B. Brinkmann, *Int. J. Legal Med.* **1993**, *106*, 81.  
[16] E. W. Marianne, *Talanta* **2001**, *54*, 427.  
[17] H. Michael, *Part. Part. Syst. Char.* **2005**, *22*, 401.  
[18] T. J. Shaw, D. Brown, J. D'Arcy, F. Liu, P. Shea, M. Sivakumar, T. Gozani, *Appl. Radiat. Isot.* **2005**, *63*, 779.  
[19] T. Keller, A. Keller, E. Tutsch-Bauer, F. Monticelli, *Forensic Sci. Int.* **2006**, *161*, 130.  
[20] D. R. Justes, N. Talaty, I. Cotte-Rodriguez, R. G. Cooks, *Chem. Commun.* **2007**, *21*, 2142.  
[21] Z. Takáts, I. Cotte-Rodriguez, N. Talaty, H. Chen, R. G. Cooks, *Chem. Commun.* **2005**, *15*, 1950.  
[22] N. Na, C. Zhang, M. Zhao, S. Zhang, C. Yang, X. Fang, X. Zhang, *J. Mass Spectrom.* **2007**, *42*, 1079.  
[23] J. C. Carter, W. E. Brewer, S. M. Angel, *Appl. Spectrosc.* **2000**, *54*, 1876.  
[24] H. Tsuchihashi, M. Katagi, M. Nishikawa, M. Tatsuno, H. Nishioka, A. Nara, E. Nishio, C. Petty, *Appl. Spectrosc.* **1997**, *51*, 1796.  
[25] A. G. Ryder, *J. Forensic Sci.* **2002**, *47*, 275.  
[26] W. E. Smith, P. C. White, C. Rodger, G. Dent, in *Handbook of Raman Spectroscopy from the Research Laboratory to the Process Line* (Eds: I. R. Lewis, H. G. M. Edwards), Marcel Dekker: New York, **2001**, p 733.  
[27] J. Akhavan, *Spectrochim. Acta* **1991**, *47A*, 1247.  
[28] C. Cheng, T. E. Kirkbride, D. N. Batchelder, R. J. Lacey, T. G. Sheldon, *J. Forensic Sci.* **1995**, *40*, 31.  
[29] I. P. Hayward, T. E. Kirkbride, D. N. Batchelder, R. J. Lacey, *J. Forensic Sci.* **1995**, *40*, 883.  
[30] M. L. Lewis, I. R. Lewis, P. R. Griffiths, *Vib. Spectrosc.* **2005**, *38*, 17.  
[31] A. C. Williams, H. G. M. Edwards, B. W. Barry, *J. Raman Spectrosc.* **1994**, *25*, 95.  
[32] W. Akhtar, H. G. M. Edwards, *Spectrochim. Acta, Part A* **1997**, *53*, 81.

- [33] E. Widjaja, R. K. Seah, *Appl. Spectrosc.* **2006**, *60*, 343.  
[34] E. Widjaja, G. H. Lim, A. An, *Analyst* **2008**, *133*, 493.  
[35] J. S. Day, H. G. M. Edwards, S. A. Dobrowski, A. M. Voice, *Spectrochim. Acta, Part A* **2004**, *60*, 1725.  
[36] E. M. A. Ali, H. G. M. Edwards, M. D. Hargreaves, I. J. Scowen, *Anal. Bioanal. Chem.* **2008**, *390*, 1159.  
[37] Z. Fang, S. Wang, F. Li, *Prop., Explos., Pyrotech.* **1998**, *23*, 317.  
[38] Y. A. Gruzdkov, Y. M. Gupta, *J. Phys. Chem.* **2001**, *105*, 6197.  
[39] I. R. Lewis, N. W. Daniel, P. R. Griffiths, *Appl. Spectrosc.* **1997**, *51*, 1854.  
[40] E. A. Carter, H. G. M. Edwards, in *Infrared and Raman Spectroscopy of Biological Materials* (Eds: H. Gremlich, B. Yan), Marcel Dekker: New York, **2001**, p 429.  
[41] G. Herzberg, *Molecular Spectra and Molecular Structure*, D. Van Nostrand Company: New York, **1945**, 179.  
[42] J. O. Jensen, *Spectrochim. Acta, Part A* **2002**, *58*, 1347.